R. & M. No. 2843
(10,616)
A.R.C. Technical Report

MINISTRY OF SUPPLY

AERONAUTICAL RESEARCH COUNCIL
REPORTS AND MEMORANDA

Low-speed Wind-tunnel Tests on a Model of a Jet Tailless Aircraft

By

J. TROUNCER, M.A.,
and
G. F. MOSS, B.Sc.

LONDON: HER MAJESTY'S STATIONERY OFFICE
1956
PRICE 9*s* 6*d* NET

Low-speed Wind-tunnel Tests on a Model of a Jet Tailless Aircraft

By

J. TROUNCER, M.A.,

and

G. F. MOSS, B.Sc.

COMMUNICATED BY THE PRINCIPAL DIRECTOR OF SCIENTIFIC RESEARCH (AIR), MINISTRY OF SUPPLY

*Reports and Memoranda No. 2843**

January, 1947

Summary.—This report gives the results of longitudinal and lateral stability tests made on a model of a jet tailless aircraft. It includes the effects of split flaps, trimming flaps, dive-recovery flaps and four types of anti-tip-stalling device (slats, nose flaps, double split flaps and letter-box slots). It also includes the effect of the ground in the landing condition.

1. *Introduction*.—Wind-tunnel tests were required to assist in the design of a jet-propelled tailless aircraft. The tests covered the standard longitudinal and lateral measurements, together with some research into the problems of flap design and the best type of anti-tip-stalling device. This report gives an account of the programme covered and full tables of the results.

2. *Details of Tests*.—The tests were made between November, 1945, and May, 1946, in the No. 1, 11½-ft Wind Tunnel at the Royal Aircraft Establishment. The majority of the measurements were made at a wind speed of 120 ft/sec, giving a Reynolds number, based on mean chord, of $1 \cdot 28 \times 10^6$; but a few tests were also made at 180 ft/sec ($R = 1 \cdot 93 \times 10^6$) to check the Reynolds number effect.

The model used for the tests was a 1/5-scale model on which the air-intake ducts were correctly represented as far as the engine and then converged to form a single duct which continued to the rear of the fuselage. The model was fitted with elevons, trimming flaps, split flaps and dive-recovery flaps and also had a removable leading edge so that it could be tested with and without fixed letter-box slots. A wire of 24 standard wire gauge was fitted around the nose of the model to fix the body transition.

A general arrangement drawing of the model is given in Fig. 1 and the model dimensions in Table 1.

All pitching-moment coefficients are given relative to the wing mean quarter-chord point.

* R.A.E. Report Aero. 2181, received 19th May, 1947.

3. *Results.*—3.1. *Lift, Longitudinal Stability and Trim.*—3.1.1. *Flaps up* (*Table* 2, *Fig.* 3).—In the basic condition with flaps up and no anti-tip-stalling devices fitted the aircraft develops a tip stall at a trimmed lift coefficient of 0·67 at $R = 1 \cdot 28 \times 10^6$ (Fig. 3). The stall is delayed to $C_L = 0 \cdot 77$ at $R = 1 \cdot 94 \times 10^6$ (Table 2) and there will clearly be a large scale effect on this and on maximum lift. The curves for $\eta_w = +15$ deg, -15 deg, -20 deg and -25 deg in Fig. 3* have been constructed from the elevon power measurements given in Table 11.

The neutral point over the range $0 < C_L < 0 \cdot 6$ is at $h_n = 0 \cdot 33$. Since the c.g. range of the aircraft is from 0·14 to 0·29 of the mean chord this gives a static margin at $R = 1 \cdot 28 \times 10^6$ of 0·04 in the aft c.g. position. The normal c.g. of the aircraft is at $0 \cdot 24\bar{c}$.

Tests made with the duct entries open and closed† showed that the only change was on maximum lift coefficient which was 0·05 greater in the closed condition. Surface tufting showed that this increase was due to the elimination of a stall which developed from the entry lip in the open condition.

Unless otherwise stated the tests described in this report were all made with the duct entries open.

3.1.2. *Effect of split flaps* (*Table* 3. *Figs.* 4 *and* 5).—The split flaps designed for this aircraft‡ gave no change in neutral point but caused a large negative change in trim (ΔC_M flaps $= -0 \cdot 048$ at $C_L = 0 \cdot 5$). Two methods of reducing this change in trim were tried:—

(*a*) by moving the flap hinge-line forward by an amount equal to the flap chord

(*b*) by reducing the flap chord to approximately half the design value (*see* Fig. 1).

The results on lift and pitching moment are summarised below and plotted, for an elevon angle of -10 deg, in Figs. 4 and 5.

Type of split flap	ΔC_L ($\alpha = 6$ deg)	$\Delta C_{M\bar{c}/4}$ ($\alpha = 6$ deg)	$\Delta C_{M\bar{c}/4}$ ($C_L = 0 \cdot 5$)	$\Delta C_{L\,max.}$
Large-chord flaps hinged in rear position	0·34	0·089	0·048	0·19
Large-chord flaps hinged in forward position	0·28	0·039	0·006	0·04
Small-chord flaps hinged in rear position	0·22	−0·055	−0·031	0·10

The lift increases given above are the untrimmed values.

Although the forward position of flap gave good results at low incidences, there was a large drop in lift over the stall with this arrangement. A few measurements made with the flaps hinged in the rear position at the inboard end and set perpendicular to the wind across the wing showed a similar loss in lift at high incidences, the pitching-moment curve in this condition being almost identical to that with the flaps hinged forward.

Halving the flap chord reduced the change of trim and lift increment due to the flaps by 35 per cent over the whole incidence range.

* η_w is the value of the elevon angle measured along wind.

† In the closed condition the entries were faired over to give the 'datum wing' leading edge shown in Fig. 1.

‡ Large chord flaps hinged in the rear position, *see* Fig. 1 and Table 1.

As there were structural difficulties associated with moving the flap forward on the full-scale aircraft the smaller-chord flap was recommended and all subsequent tests were made with this type of flap.

The maximum trimmed lift coefficient in this condition is $C_L = 0 \cdot 94$ ($R = 1 \cdot 28 \times 10^6$), with instability setting in at $C_L = 0 \cdot 78$ (Fig. 5).

3.1.3. *Effect of trimming flaps* (*Tables* 2 *and* 3. *Figs.* 6, 7 *and* 8).—In the original design a trimming flap was incorporated which extended inboard from the elevon (*see* Fig. 1). This was designed to be deflected to small negative angles when the split flaps were down and it was hoped that this might provide the necessary change in trim without unduly affecting the lift due to the flaps.

In fact, as Figs. 6, 7 and 8 show, the trimming flaps gave, in comparison with the elevons, a large change in lift and only a relatively small change in trim. It was also found that the effects of the trimming flaps were reduced to less than one-half on opening the split flaps. To investigate this point further, some tests were made with the split flaps raised off the wing by 1/3 of the flap chord to allow the air free passage over the trimming flap. Although this increased the efficiency of the trimming flaps, the raising of the split flaps caused a further negative change in trim and there was little net gain.

For the results given in Figs. 6, 7 and 8 and except where specifically stated to the contrary in the tables* the split-flap angle was fixed relative to the wing and did not move when the trimming flap was raised.

3.1.4. *Effect of dive-recovery flaps* (*Table* 4. *Fig.* 9).—The dive-recovery flaps shown in Fig. 1 were found to give a negative pitching moment instead of the required positive increment. At $C_L = 0$, $\Delta C_M = -0 \cdot 015$ but this reduced to $\Delta C_M = 0$ by $C_L = 0 \cdot 6$ (Fig. 9). A reduction of the flap span was found to have no effect.

A single measurement was taken with the flaps moved back from their design position at $0 \cdot 77c$ to $0 \cdot 40c$ but, as the pitching moment lay on the original curve with flaps up no further tests were made.

3.1.5. *Tests with ground represented* (*Table* 6. *Fig.* 10).—To cover the landing condition some tests were made with the ground represented. For these the model was fitted with 74 per cent span slats and suspended so that the jet exit was just clear of the ground at an incidence of 20 deg.

Fig. 10 gives a comparison of the results with and without ground and shows that the ground effect was relatively small. It caused a positive change of trim ($\Delta C_M \simeq 0 \cdot 01$ with elevons at 0 deg) and tended to destabilize the aircraft at high incidences with flaps down, but both these effects became less as negative elevon was applied.

3.2. *Anti-Tip-Stalling Devices* (*Tables* 5 *to* 9).—One of the foremost problems associated with all swept-back wings is to find a satisfactory method of curing the tip-stalling tendencies at low speeds without detracting too much from the high-speed qualities of the wing. On this model four types of anti-stalling device were tested, namely:—

* *Viz.* in Tables 6 and 10.

(*a*) Handley Page slats

(*b*) nose flaps

(*c*) double split flaps

(*d*) letter-box slots.

The effect of (*a*), (*b*) and (*c*) have been discussed already in Ref. 1, but, as no tables of results were given, these have been included in the present report.

Some further tests were also made besides those recorded in Ref. 1 and the results of these are given briefly below.

3.2.1. *Constant-chord nose flaps* (*Table* 7B).—The nose flaps described in Ref. 1 were tapered flaps of chord equal to 10 per cent of the local wing chord.

Tests made with a 50 per cent span nose flap of constant chord equal to 0·83 ft full-scale* gave almost identical results to those made with the tapered nose flap of the same span.

3.2.2. *Small-chord double split flaps* (*Table* 8B. *Fig.* 11).—The double split flaps of Ref. 1 covered 2/3 of the elevon chord (*see* Fig. 2b). Some smaller flaps of only 1/5 of the elevon chord were also tested and Fig. 11 gives a comparison of the effects obtained with the two sizes of flap.

It will be seen that the smaller flaps were less favourable as they gave instability near the stall, though this was reduced when negative elevon was applied. Also the slope of the pitching-moment curves at lower lift coefficients was as excessive with the small flaps as with the large, though there was less change of trim.

3.2.3. *Letter-box slots* (*Tables* 9A *and* 9B. *Fig.* 12).—Fig. 2a gives sections of the letter-box slots tested and the results for the various slot spans are given in Table 9A. It was found that the results varied only slightly with change of span and in no case was the tip stall cured. It was thought that this might be due to the rather small gap of the original design (approx. 1 per cent of the chord) and further tests were therefore made with a modified slot which had a gap of 2 per cent of the chord (Table 9B). Fig. 12 gives the results with the two types of slot and shows that the increase in slot gap gave no improvement over the original design.

3.2.4. *Profile drags* (*Fig.* 13).—The increases in profile drag due to the fitting of anti-tip-stalling devices were not given in Ref. 1, but form an important factor on an aircraft designed specifically for high speed. Fig. 13 gives profile-drag comparisons at an elevon angle of —10 deg, showing the effect of opening slats, nose flaps or double split flaps on this model.

At small lift coefficients the increase in profile-drag coefficient due to slats or nose flaps was about 0·005 but, above $C_L = 0 \cdot 5$, it became negative because of the elimination of the tip stall. The drag figures with nose flap have been corrected by the aid of Table 2 to allow for the fact that the duct entries were closed in this case.

Fig. 13 shows clearly the large drag increases which were caused by the double split flaps even at lift coefficients greater than 0·5.

* This gives a nose-flap chord/wing chord ratio of 20·4 per cent at the tip and 9·6 per cent inboard.

3.3. *Lateral and Directional Stability* (*Table* 10. *Figs.* 14 *to* 18).—In all the lateral tests, measurements were made at positive and negative angles of sideslip. At low incidences the curves obtained were symmetrical, and the values at positive and negative angles of sideslip have been meaned and the derivatives taken over the range $\beta = \pm 2 \cdot 5$ deg. The values of n_v, l_v and y_v obtained are plotted in Figs. 14, 15 and 16.

Above $\alpha = 9 \cdot 85$ deg the yawing-moment curves became unsymmetrical, and unstable at some angles of yaw, as shown in Fig. 17. The side-force curves were similarly affected but the changes in rolling moment were comparatively slight.

Detailed tests made on a 45-deg swept-back wing of aspect ratio $3 \cdot 0$ and taper ratio 4 : 1 (Model B, Ref. 2) have since shown that this type of yawing-moment curve is liable to occur on any swept-back wing at incidences near the tip-stalling incidence. It is due to transition from a symmetrical curve to one of two alternative subsidiary 'loops' which can be obtained if one or the other wing tip is caused to stall prematurely. On this particular model the accumulative errors in the model and the tunnel flow caused a tendency for the port wing to stall first, as is shown by the large negative yawing moments at $\beta = 0$ deg (Fig. 17).

The only means of eliminating the risk of such directional instability is to delay the tip stall by some means. Fig. 18 shows how the curves were improved by fitting the 37 per cent span slats. In this case there was only slight asymmetry at the highest incidences and up to $\alpha = 15$ deg the curves were straight and symmetrical.

The fin effect on n_v and y_v was as follows:—

$$\Delta n_v \text{ (fin)} = 0 \cdot 04$$

$$\Delta y_v \text{ (fin)} = -0 \cdot 105 .$$

3.4. *Controls.*—3.4.1. *Elevon power* (*Table* 11. *Figs.* 16, 17 *and* 18).—Elevon power was measured over a range of incidence on the plain wing, flaps 0 deg, and at the highest incidence with 74 per cent span slats fitted.

The results are given in Table 11 and the increments of pitching moment, yawing moment and rolling moment are plotted in Figs. 16, 17 and 18.

There was a steady decrease in elevon effectiveness as the angle of attack was increased and this was only partly restored by opening the slats (Fig. 16).

The following table gives the rolling moment and adverse yawing moment produced by elevon movements of ± 15 deg from their position for trimmed flight at various lift coefficients.

C_L trimmed	Port elevon 15 deg down, Starboard elevon 15 deg up } from trimmed position	
	$10^3 \Delta C_n$	$10^3 \Delta C_l$
No slats		
0·4	−0·1	55
0·45	−0·5	48
0·70	−4·1	37
With 74 per cent span slats		
0·70	−0·8	49

Only at the highest incidences does the adverse yawing moment become appreciable, and this is reduced, and the rolling moment considerably increased, by opening the slats.

3.4.2. *Rudder power* (*Table* 12).—Rudder power was measured at $C_L = 0 \cdot 05$ and Table 12 gives the results on yaw and side force for rudder angles of 0 deg to 20 deg. The variation with rudder angle was found to be linear and the rudder power was as follows:—

$$10^3\,\Delta C_n = -0 \cdot 38 \text{ per degree of rudder angle.}$$

$$10^3\,\Delta C_y = 1 \cdot 64 \text{ per degree of rudder angle.}$$

REFERENCES

No.	*Author*	*Title, etc.*
1	J. Trouncer	A comparison of the effects of slats, nose flaps and double split flaps on a model of a 40-deg swept-back tailless aircraft. A.R.C. 9980. June, 1946. (Unpublished).
2	J. Trouncer	Wind-tunnel tests to investigate directional asymmetry and instability on a swept-back wing (Model B, 45-deg sweepback, aspect ratio 3). A.R.C. 10,489. January, 1947. (Unpublished).

TABLE 1

Model Data

Scale of model, 1/5th

		Model-Scale	Full-Scale
Wing			
Area*	S	13·27 sq ft	331·6 sq ft
Span	b	7·8 ft	39 ft
Mean chord	$\bar{c}$	1·701 ft	8·505 ft
Aspect ratio	A	4·59	
Section		EQ 10 40 symmetrical	
Chord at AA		9·8 in.	4·08 ft
at BB (4·83 ft full-scale from centre-line)		26 in.	10·83 ft
Sweepback of 25 per cent chord line between AA and BB		40 deg	
Dihedral		0 deg	
Geometric twist		0 deg	
Mean quarter-chord point position (on chord-line)			
Distance aft of leading edge at BB		12·74 in.	5·31 ft
Elevons			
Span		1·90 ft	9·50 ft
Area aft of hinge		0·61 sq ft	15·25 sq ft
Chord aft of hinge at AA		3·6 in.	1·50 ft
at XX		4·1 in.	1·71 ft
η_w = elevon angle measured along wind			
Trimming flaps			
Span		1·41 ft	7·07 ft
Area aft of hinge		0·56 sq ft	14·07 sq ft
Chord aft of hinge at XX		4·1 in.	1·71 ft
at BB		4·37 in.	1·82 ft
at CC		8·87 in.	3·70 ft
Split flaps			
Span		1·41 ft	7·07 ft
Angle (about hinge-line)		60 deg	
(along wind)		51 deg 14 sec	
(*a*) Large-chord flaps			
Area†		72·2 sq in.	12·50 sq ft
Chord at XX	C_f	4·1 in.	1·71 ft
at CC	C_f	4·5 in.	1·88 ft
(*b*) Small-chord flaps			
Area†		34·0 sq in.	5·90 sq ft
Chord at XX	C_f	1·90 in.	0·79 ft
at CC	C_f	2·08 in.	0·87 ft

* Based on projected leading-edge and trailing-edge lines (*i.e.*, omitting the fillet) to fuselage side, then straight across the centre-section.

† This area allows for the cut-out which is necessary at station BB.

TABLE 1—*continued*

	Model-Scale	*Full-Scale*
Position of flap hinge		
For rear position this is distance C_f from the wing trailing edge.		
For forward position this is distance $2 \times C_f$ from the wing trailing edge.		
Dive-recovery flaps		
Inboard portion Span	4·2 in.	1·75 ft
Area	3·78 sq in.	0·655 sq ft
Angle (about hinge-line)	90 deg	
Outboard portion Span	9·7 in.	4·04 ft
Area	11·3 sq in.	1·96 sq ft
Angle (about hinge-line)	90 deg	
Fin and rudder		
Gross area* S'' per cent	1·51 sq ft	37·85 sq ft
Sweepback of 25 per cent chord line to vertical	48 deg	
Fin arm (Mean quarter-chord point wing to mean quarter-chord point fin and rudder) l''	18·04 in.	7·51 ft
Volume coefficient $\bar{V}'' \dfrac{S''l''}{Sb}$	0·022	
Handley Page slats		
Span/semi-span	0·37 and 0·74	
Nose flaps		
Tapered: span/semi-span	0·37, 0·50, 0·74 and 0·89	
Constant chord: span/semi-span	0·50	
Chord	2 in.	0·83 ft
Double split flaps (*see* Fig. 2)		
(*a*) Large-chord flaps		
Span/elevon span	0·73 and 1·00	
Chord/elevon chord	0·667	
Angle (about hinge-line)	60 deg and 40 deg	
(*b*) Small-chord flaps		
Span/elevon span	0·61 and 1·00	
Chord/elevon chord	0·20	
Angle (about hinge-line)	60 deg	
Letter-box slots (*see Fig.* 2)		
Design slots with gap $\simeq$ 1 per cent chord		
Span/semi-span	0·18, 0·29, 0·48 and 0·73	
Revised slots with gap $\simeq$ 2 per cent chord		
Span/semi-span	0·48	

* Based on projected leading-edge and trailing-edge lines to fuselage, then across fuselage at right-angles to fuselage datum-line.

TABLE 2

Lift, Drag and Pitching-Moment Coefficients
Flaps 0 deg

Complete model. Plain wing.

η_w (deg)	Trimming flaps	α (deg)	C_L	C_D	$C_{M\bar{c}/4}$
V = 180 ft/sec $R = 1 \cdot 93 \times 10^6$ With duct entries blocked					
0	0	0·4	0·010	0·0096	−0·0031
		2·55	0·138	0·0118	−0·0126
		6·75	0·399	0·0244	−0·0330
		11·0	0·649	0·0500	−0·0499
		13·1	0·778	0·0895	−0·0609
		15·2	0·855	0·1514	−0·0410
		17·2	0·894	0·2175	−0·0213
V = 120 ft/sec $R = 1 \cdot 28 \times 10^6$ With duct entries blocked					
0	0	−1·8	−0·117	0·0114	−0·0012
		0·3	0·009	0·0099	−0·0050
		2·4	0·136	0·0116	−0·0119
		4·55	0·264	0·0165	−0·0216
		6·65	0·397	0·0245	−0·0325
		8·75	0·521	0·0358	−0·0410
		10·9	0·653	0·0643	−0·0532
		13·0	0·763	0·106	−0·0526
		15·05	0·843	0·157	−0·0363
		17·1	0·892	0·216	−0·0205
		19·15	0·929	0·275	−0·0135
		21·15	0·950	0·332	−0·0229
		23·15	0·951	0·388	−0·0377
		25·15	0·948	0·438	−0·0654
		27·15	0·948	0·485	−0·0830
		28·15	0·932	0·504	−0·0927
V = 120 ft/sec With duct entries open					
0	0	−1·8	−0·126	0·0123	0·0082
		2·4	0·116	0·0118	−0·0115
		6·65	0·382	0·0243	−0·0327
		10·9	0·648	0·0680	−0·0543
		13·0	0·740	0·104	−0·0536
		15·05	0·818	0·165	−0·0354
		17·1	0·889	0·227	−0·0224
		19·15	0·908	0·274	−0·0063
		21·1	0·899	0·341	−0·0337
		23·1	0·901	0·396	−0·0648
		25·1	0·894	0·438	−0·0858

TABLE 2—*continued*

η_w (deg)	Trimming flaps	α (deg)	C_L	C_D	$C_{M\bar{c}/4}$
10	0	2·3	0·006	0·0145	0·0785
		6·55	0·282	0·0219	0·0479
		10·8	0·545	0·5032	0·0169
		12·9	0·668	0·0942	0·0050
		15·0	0·743	0·154	0·0187
		17·05	0·821	0·212	0·0296
		19·05	0·840	0·265	0·0367
		21·05	0·822	0·321	0·0106
		23·05	0·821	0·367	−0·0146
0	10	2·25	−0·035	0·0126	0·0332
		6·5	0·242	0·0192	0·0074
		10·75	0·478	0·0423	−0·0132
		12·85	0·599	0·0774	−0·0208
		14·95	0·707	0·136	0·0005
		17·0	0·786	0·193	0·0240
		19·05	0·822	0·244	0·0042
		21·05	0·815	0·308	−0·0138
		23·05	0·826	0·350	−0·0130

TABLE 3

Lift, Drag and Pitching-Moment Coefficients with Split Flaps at 60 deg

Complete model. Plain wing. Entries open. V = 120 ft/sec.

Type of split flap*	η_w (deg)	Trimming flaps	α (deg)	C_L	C_D	$C_{M\,\bar{c}/4}$
Large-chord flaps: hinged in rear position	−10	0	0·5	0·240	0·0793	0·0052
			4·75	0·501	0·0924	−0·0236
			9·0	0·782	0·132	−0·0631
			11·1	0·901	0·176	−0·0802
			13·2	0·981	0·244	−0·0738
			15·25	1·032	0·304	−0·0579
			17·25	1·032	0·357	−0·0464
			19·25	1·022	0·425	−0·0756
			21·25	1·022	0·478	−0·0942
Large-chord flaps: hinged in forward position	−10	0	0·5	0·203	0·0862	0·0503
			4·7	0·450	0·0923	0·0243
			8·95	0·689	0·124	−0·0067
			11·05	0·815	0·167	−0·0221
			13·1	0·866	0·225	−0·0094
			15·1	0·887	0·275	0·0096
			17·1	0·883	0·317	0·0435
			19·05	0·836	0·373	0·0213
Large-chord flaps: hinged in rear position at inboard end and set perpendicular to wind across wing	−10	0	4·5	0·496	0·104	0·0136
			8·7	0·734	0·132	−0·0102
			10·8	0·845	0·175	−0·0222
			12·85	0·884	0·235	−0·0118
			14·85	0·884	0·287	+0·0116
Small-chord flaps: hinged in rear position	−10	0	0·4	0·121	0·0478	0·0344
			4·65	0·385	0·0576	0·0067
			8·9	0·643	0·0854	−0·0251
			11·0	0·780	0·123	−0·0450
			13·1	0·870	0·182	−0·0404
			15·15	0·923	0·238	−0·0268
			17·15	0·940	0·287	0·0053
			19·15	0·921	0·343	−0·0071
	−10	−10†	4·3	0·287	0·0583	0·0285
			8·55	0·549	0·0765	−0·0013
			10·65	0·674	0·102	−0·0185
			12·8	0·812	0·158	−0·0323
			14·85	0·884	0·223	−0·0248
			16·9	0·929	0·279	−0·0046
			18·9	0·915	0·341	−0·0047

* For flap chord and flap hinge-line position *see* Table 1.

† The split-flap angle was fixed relative to the wing and did not move when the trimming flap was raised.

TABLE 3—*continued*

Type of split flap*	η (deg)	Trimming flaps	α (deg)	C_L	C_D	$C_{M\bar{c}/4}$
Small-chord flaps: hinged in rear position and raised one-third of flap chord above wing	10	0	4·4	0·371	0·0621	0·0016
			8·6	0·619	0·0838	0·0258
			10·75	0·761	0·117	0·0455
			12·85	0·868	0·173	−0·0507
			14·9	0·942	0·236	−0·0363
			16·95	0·961	0·288	0·0203
			18·9	0·928	0·348	−0·0161
	10	10†	4·3	0·281	0·0665	0·0278
			8·4	0·408	0·0720	0·0187
			10·55	0·531	0·0821	0·0059
			12·65	0·666	0·109	0·0131
			14·8	0·798	0·161	0·0221
			16·85	0·873	0·225	0·0171
			18·9	0·921	0·279	0·0022
			20·9	0·913	0·331	0·0122

* For flap chord and flap hinge-line position *see* Table 1.

† The split-flap angle was fixed relative to the wing and did not move when the trimming flap was raised.

TABLE 4

Lift, Drag and Pitching-Moment Coefficients with Dive-Recovery Flaps Open

Complete model. Plain wing. Entries open. $V = 120$ ft/sec.
Trimming flap 0 deg. $\eta_w = 0$ deg.

Dive-recovery flap position	α (deg)	C_L	C_D	$C_{M\bar{c}/4}$
With flaps in design position (Hinged at 0·077*c* approx.)	0·3	0·021	0·0285	−0·0186
	2·45	0·142	0·0261	−0·0253
	4·55	0·262	0·0276	−0·0317
	6·65	0·389	0·0327	−0·0405
	8·75	0·508	0·0428	−0·0468
With flaps hinged at 0·40*c*	5·6	0·337	0·0284	−0·0269
With reduced span flaps‡ hinged at 0·077*c*	5·6	0·327	0·0283	−0·0346
With reduced span flaps hinged at 0·161*c*	5·6	0·332	0·0308	0·0347

‡ For the reduced span flaps the length of the swept back portion was shortened at the outboard end by 4·8 in. model-scale, *i.e.*, 2 ft full-scale.

TABLE 5

Lift, Drag and Pitching-Moment Coefficients with Handley Page Slats

Complete model. Entries open. $V = 120$ ft/sec.

Slat span from tip / Semi-span	η_w (deg)	Trimming flaps	α (deg)	C_L	C_D	$C_{M\,\bar{c}/4}$
Flaps 0 deg						
0·37	0	0	0·3	−0·023	0·0167	0·0022
			4·5	0·224	0·0207	−0·0111
			8·75	0·476	0·0364	−0·0352
			10·85	0·598	0·0504	−0·0483
			12·95	0·716	0·0733	−0·0540
			15·05	0·822	0·113	−0·0572
			17·15	0·911	0·175	−0·0623
			18·15	0·954	0·223	−0·0732
			19·2	0·960	0·267	−0·1037
	−10	0	4·4	0·130	0·0210	0·0586
			8·65	0·387	0·0331	0·0386
			10·75	0·504	0·0444	0·0255
			12·85	0·627	0·0650	0·0143
			15·0	0·740	0·102	0·0056
			17·05	0·838	0·170	−0·0069
			19·1	0·860	0·242	−0·0438
0·74	0	0	−0·1	−0·025	0·0217	−0·0053
			3·05	0·157	0·0231	−0·0059
			7·3	0·413	0·0347	−0·0272
			9·4	0·546	0·0458	−0·0413
			11·5	0·672	0·0626	−0·0516
			13·6	0·788	0·0847	−0·0598
			15·7	0·900	0·113	−0·0674
			17·8	1·010	0·156	−0·0771
			19·85	1·067	0·220	−0·0758
			21·9	1·112	0·289	−0·0707
			23·95	1·135	0·355	−0·0780
			26·9	1·105	0·435	−0·0734
0·74	−10	0	2·95	0·054	0·0236	0·0558
			7·2	0·304	0·0310	0·0432
			9·3	0·428	0·0384	0·0321
			11·4	0·559	0·0516	0·0203
			13·5	0·677	0·0698	0·0099
			15·6	0·794	0·0939	−0·0001
			17·75	0·906	0·129	−0·0135
			19·8	0·994	0·196	−0·0230
			21·85	1·033	0·261	−0·0246
			23·85	1·060	0·331	−0·0323
			25·85	1·033	0·380	−0·0264
	0	−10	2·9	−0·002	0·0224	0·0293
			5·0	0·116	0·0250	0·0275
			9·25	0·369	0·0347	0·0020

TABLE 5—*continued*

Slat span from tip / Semi-span	η_{tr} (deg)	Trimming flaps	α (deg)	C_L	C_D	$C_{M\,\bar{c}/4}$
Flaps 60 deg (Small-chord flaps hinged in rear position)						
0·37	0	0	8·95	0·721	0·0837	0·0909
			11·05	0·843	0·106	0·1008
			13·15	0·946	0·139	0·1025
			15·25	1·041	0·203	−0·1058
			17·25	1·058	0·268	−0·1098
			19·25	1·062	0·338	0·1385
	10	0	0·4	0·102	0·0519	0·0285
			4·65	0·358	0·0604	0·0109
			8·85	0·620	0·0806	0·0159
			11·0	0·745	0·0986	0·0301
			13·1	0·871	0·131	0·0447
			15·2	0·968	0·186	0·0555
			17·2	0·986	0·255	0·0621
			19·2	0·990	0·320	0·0904
	15	0	0·3	0·023	0·0582	0·0635
			4·55	0·288	0·0628	0·0469
			8·8	0·546	0·0795	0·0231
			10·9	0·676	0·0952	0·0077
			13·05	0·815	0·124	0·0106
			15·15	0·931	0·183	−0·0295
			17·15	0·951	0·242	0·0347
			19·15	0·953	0·310	0·0633
	20	0	13·0	0·778	0·128	0·0189
			15·1	0·884	0·176	−0·0010
			17·15	0·919	0·235	−0·0089
			19·15	0·913	0·300	−0·0385
	15	15*	4·45	0·151	0·0545	0·0764
			8·7	0·412	0·0655	0·0533
			10·8	0·554	0·0790	0·0361
			12·95	0·691	0·106	0·0185
			15·05	0·825	0·151	0·0002
			17·15	0·920	0·221	0·0178
			19·15	0·944	0·293	−0·0637
			20·15	0·953	0·322	0·0825
0·74	0	0	0·1	0·193	0·0487	0·0468
			3·25	0·384	0·0578	−0·0577
			7·5	0·646	0·0776	−0·0831
			9·6	0·779	0·0942	−0·0953
			11·75	0·910	0·116	−0·1045
			13·85	1·021	0·140	0·1102
			15·9	1·120	0·174	0·1127
			18·0	1·180	0·231	−0·0923
			20·0	1·195	0·294	−0·0717
			22·0	1·201	0·361	−0·0677
			24·0	1·177	0·418	−0·0620

* The split flaps were fixed relative to the wing and did not move when the trimming flaps were raised.

TABLE 5—*continued*

Slat span from tip / Semi-span	η_w (deg)	Trimming flaps	α (deg)	C_L	C_D	$C_{M\,\bar{c}/4}$
Flaps 60 deg—*continued*						
0·74	−10	0	3·15	0·287	0·0551	0·0118
			7·4	0·522	0·0751	−0·0043
			9·5	0·660	0·0882	−0·0168
			11·6	0·784	0·106	0·0282
			13·75	0·908	0·127	−0·0386
			15·85	1·030	0·162	−0·0506
			17·9	1·120	0·215	−0·0462
			19·95	1·143	0·278	−0·0318
			21·95	1·144	0·341	−0·0247
	−20	0	9·4	0·548	0·0907	0·0573
			11·5	0·679	0·106	0·0458
			13·65	0·811	0·126	0·0313
			15·75	0·926	0·153	0·0180
			17·85	1·028	0·195	0·0068
			19·9	1·073	0·269	0·0120
			21·9	1·086	0·325	0·0125
	−10	−10*	9·45	0·604	0·0872	−0·0028
			11·55	0·725	0·104	−0·0147
			13·7	0·860	0·127	−0·0269
			15·8	0·990	0·158	−0·0389
			17·9	1·090	0·206	−0·0429
			19·95	1·140	0·278	−0·0238

* The split flaps were fixed relative to the wing and did not move when the trimming flaps were raised.

TABLE 6

Lift, Drag and Pitching-Moment Coefficients with the Ground Represented

Complete model with 74 per cent span slats. Entries open. $V = 120$ ft/sec.

Condition of model	η_w (deg)	Trimming flaps	α (deg)	C_L	C_D	$C_{M\bar{c}/4}$
Flaps 0 deg	0	0	4	0·236	0·0220	−0·0060
			8	0·532	0·0307	−0·0322
			10	0·675	0·0416	−0·0431
			12	0·796	0·0567	−0·0499
			14	0·917	0·0816	−0·0589
			16	1·021	0·131	−0·0706
			18	1·101	0·206	−0·0838
			19	1·149	0·242	−0·0929
	−10	0	4	0·138	0·0232	0·0627
			8	0·432	0·0284	0·0363
			10	0·568	0·0361	0·0249
			12	0·712	0·0505	0·0095
			14	0·833	0·0708	−0·0024
			16	0·943	0·113	0·0192
			18	1·014	0·172	−0·0419
Flaps 60 deg relative to trimming flaps (small-chord flaps hinged in rear position)	−10	0	4	0·407	0·0599	0·0102
			8	0·664	0·0640	−0·0110
			10	0·795	0·0728	−0·0226
			12	0·914	0·0890	−0·0339
			14	1·016	0·116	−0·0370
			16	1·073	0·170	−0·0286
			18	1·123	0·242	0·0335
			19	1·142	0·274	−0·0346
Flaps 60 deg relative to trimming flaps (small-chord flaps hinged in rear position)	−15	0	12	0·867	0·0893	0·0014
			14	0·978	0·114	−0·0085
			16	1·049	0·175	0·0076
			18	1·099	0·242	−0·0108
			19	1·114	0·277	−0·0133
	−20	0	4	0·298	0·0673	0·0787
			8	0·570	0·0720	0·0622
			10	0·705	0·791	0·0478
			12	0·819	0·0899	0·0333
			14	0·938	0·115	0·0189
			16	1·020	0·173	0·0134
			18	1·068	0·242	0·0076
			19	1·086	0·270	0·0054
	−15	−15	4	0·203	0·0567	0·0789
			8	0·477	0·0602	0·0573
			10	0·625	0·0674	0·0448
			12	0·768	0·0803	0·0261
			14	0·881	0·0993	0·0115
			16	1·007	0·155	−0·0005
			18	1·064	0·219	−0·0036
			19	1·087	0·249	−0·0070

TABLE 6—*continued*

Condition of model	η_w (deg)	Trimming flaps	α (deg)	C_L	C_D	$C_{M\,\bar{c}/4}$
Flaps 60 deg (large-chord flaps hinged in forward position)	−10	0	4	0·498	0·0871	0·0247
			8	0·734	0·0920	0·0043
			10	0·842	0·0991	−0·0039
			12	0·937	0·114	−0·0088
			14	1·004	0·151	−0·0004
			16	1·039	0·212	0·0084
			18	1·052	0·269	0·0088
			19	1·058	0·305	0·0061

TABLE 7A

Lift, Drag and Pitching-Moment Coefficients with Nose Flaps (tapered)

Complete model. Trimming flaps 0 deg. $V = 120$ ft/sec.

Nose flap span from tip / Semi-span	η_w (deg)	α (deg)	C_L	C_D	$C_{M\,\bar{c}/4}$
Flaps 0 deg. Entries closed*					
0·37	0	8·75	0·491	0·0343	−0·0378
		13·0	0·743	0·0713	−0·0463
		15·1	0·869	0·121	−0·0600
		17·15	0·958	0·192	−0·0775
		19·25	1·018	0·260	−0·1058
		21·25	1·053	0·311	−0·1254
0·50	0	8·75	0·497	0·0360	−0·0376
		13·0	0·747	0·0687	−0·0457
		15·1	0·870	0·104	−0·0544
		17·2	0·989	0·172	−0·0810
		19·25	1·066	0·245	−0·1093
		21·3	1·085	0·310	−0·1534
	−10	8·65	0·383	0·0311	0·0397
		12·9	0·642	0·0565	0·0230
		15·0	0·765	0·0845	0·0118
		17·1	0·876	0·142	−0·0132
		19·15	0·947	0·218	−0·0476
		21·15	0·951	0·267	0·0802
0·74	0	13·0	0·753	0·0633	−0·0423
		15·1	0·882	0·0873	−0·0441
		17·2	1·002	0·120	0·0530
		19·3	1·116	0·170	−0·0402
		21·35	1·176	0·214	0·0195
0·89	0	4·5	0·220	0·0307	−0·0442
		8·75	0·505	0·0412	0·0460
		13·0	0·757	0·0646	−0·0423
		15·1	0·872	0·0831	−0·0384
		16·15	0·952	0·101	0·0456
		17·2	1·003	0·116	−0·0437
		19·3	1·110	0·157	−0·0270
		21·4	1·198	0·209	−0·0027
		23·45	1·278	0·277	0·0161
		25·5	1·303	0·364	0·0204
		27·45	1·282	0·445	0·0152
Flaps 0 deg. Entries open					
0·50	0	8·75	0·503	0·0387	0·0415
		12·95	0·728	0·0738	−0·0466
		15·05	0·845	0·112	−0·0500
		17·15	0·957	0·174	−0·0723
		19·25	1·015	0·263	−0·1298

* The graphs of Ref. 1 were corrected for the sake of comparison to the 'entries open' condition.

TABLE 7A—*continued*

Nose flap span from tip / Semi-span	η_w (deg)	α (deg)	C_L	C_D	$C_{M\,\bar{c}/4}$
Flaps 60 deg (small-chord flaps hinged in rear position)					
Entries closed					
0·37	0	8·95	0·734	0·0803	−0·0893
		13·2	0·972	0·135	−0·0983
		15·25	1·050	0·206	−0·1112
		17·25	1·063	0·268	−0·1237
0·50	0	9·0	0·747	0·0820	−0·0912
		13·2	0·977	0·126	−0·0947
		15·3	1·089	0·172	−0·1005
		17·35	1·169	0·240	−0·1138
		19·4	1·188	0·311	−0·1318
		21·4	1·184	0·381	−0·1668
	−10	4·6	0·342	0·0625	0·0104
		8·85	0·611	0·0762	−0·0063
		13·1	0·881	0·114	−0·0291
		15·25	1·025	0·162	−0·0503
		17·3	1·103	0·225	−0·0611
		19·35	1·128	0·302	−0·0857
	20	8·75	0·498	0·0803	0·0599
		10·9	0·641	0·0921	0·0482
		13·0	0·782	0·112	0·0298
		15·15	0·947	0·155	−0·0005
		17·25	1·042	0·220	−0·0164
		19·25	1·067	0·285	−0·0377
0·89	0	8·95	0·735	0·0825	−0·0879
		13·2	0·992	0·117	−0·0881
		15·35	1·131	0·144	−0·0912
		17·45	1·240	0·181	−0·0829
		19·5	1·293	0·228	−0·0460
		21·5	1·308	0·291	−0·0178
		23·55	1·350	0·369	−0·0123
		25·5	1·340	0·445	−0·0026

TABLE 7B

Lift, Drag and Pitching-Moment Coefficients with Nose Flaps (constant chord)

Complete model. Entries closed. Trimming flaps 0 deg. $V = 120$ ft/sec.

Nose flap span from tip / Semi-span	η_w (deg)	α (deg)	C_L	C_D	$C_{M\,\bar{c}/4}$
Flaps 0 deg					
0·50	0	4·5	0·205	0·0305	0·0197
		8·75	0·489	0·0400	0·0393
		13·0	0·754	0·0725	0·0462
		15·1	0·867	0·103	0·0497
		17·2	0·981	0·166	0·0693
		19·25	1·057	0·234	0·1038
		21·3	1·093	0·297	0·1485
	10	4·05	0·079	0·0326	0·0159
		8·65	0·382	0·0357	0·0308
		12·9	0·655	0·0615	0·0159
		15·0	0·773	0·0895	0·0103
		17·1	0·890	0·148	0·0128
		19·2	0·966	0·217	0·0498
		21·2	0·990	0·276	0·0960
Flaps 60 deg (small-chord flaps hinged in rear position)					
0·50	0	2·6	0·305	0·0614	0·0551
		4·7	0·462	0·0659	0·0699
		8·95	0·735	0·0842	0·0907
		13·2	0·986	0·131	0·0938
		15·3	1·090	0·173	0·0951
		17·4	1·183	0·241	0·112
		19·4	1·217	0·312	0·137
	−10	4·6	0·336	0·0674	0·0052
		8·85	0·618	0·0803	0·0153
		13·1	0·891	0·121	0·0352
		15·25	1·016	0·161	0·0472
		17·35	1·123	0·224	0·0646
		19·35	1·141	0·298	0·0924

TABLE 8A

Lift, Drag and Pitching-Moment Coefficients with Double Split Flaps (large chord)

Complete model. Entries open. Split flaps 0 deg. Trimming flaps 0 deg.
V = 120 ft/sec.

Double split flap span / Elevon span	Flap angle upper flap	Flap angle lower flap	η_w (deg)	α (deg)	C_L	C_D	$C_{M\,\bar{c}/4}$
1·00	60	60	−10	4·45	0·171	0·120	0·0101
				6·6	0·302	0·123	−0·0037
				8·7	0·443	0·130	−0·0236
				10·85	0·594	0·147	−0·0559
				13·0	0·785	0·185	−0·1075
				15·15	0·951	0·240	−0·1403
				17·25	1·057	0·298	−0·1413
				19·3	1·104	0·366	−0·1421
	60	0	0	12·85	0·600	0·0985	0·0211
				15·0	0·779	0·152	−0·0174
				17·1	0·879	0·211	−0·0199
				19·15	0·911	0·279	−0·0210
				21·15	0·915	0·345	−0·0524
			−10	8·45	0·188	0·0688	0·1569
				12·75	0·509	0·0945	0·0852
				14·95	0·692	0·139	0·0390
				17·05	0·807	0·197	0·0271
				19·05	0·839	0·257	0·0221
				21·05	0·843	0·312	0·0060
	0	60	−20	8·8	0·530	0·0705	−0·0685
				13·05	0·846	0·143	−0·1345
				15·2	0·960	0·203	−0·1381
				17·25	1·037	0·270	−0·1237
				19·25	1·055	0·346	−0·1146
	60	40	−10	12·95	0·737	0·153	−0·0710
				15·1	0·896	0·205	−0·1034
				17·2	1·004	0·261	−0·1071
				19·25	1·054	0·329	−0·1093
				21·25	1·065	0·400	−0·1384
0·73	60	40	−10	12·95	0·698	0·133	−0·0490
				15·1	0·859	0·185	−0·0825
				17·15	0·957	0·243	−0·0822
				19·2	1·008	0·313	−0·0787
				21·25	1·015	0·386	−0·1072
1·00 (Flap hinge moved forward to lie along elevon hinge-line)	60	0	0	12·85	0·599	0·102	0·0203
				15·0	0·781	0·155	−0·0186
				17·1	0·885	0·212	−0·0201
				19·15	0·924	0·284	−0·0245
				21·15	0·918	0·337	−0·0525
	40	0	0	12·9	0·647	0·0942	−0·0057
				15·05	0·810	0·156	−0·0301
				17·1	0·889	0·212	−0·0243
				19·15	0·910	0·279	−0·0180
				21·15	0·914	0·347	−0·0501

TABLE 8B

Lift, Drag and Pitching-Moment Coefficients with Double Split Flaps (small chord)

Complete model. Entries open. Split flaps 0 deg. Trimming flaps 0 deg.
$V = 120$ ft/sec.

Double split flap span / Elevon span	Flap angle upper flap	Flap angle lower flap	η_w (deg)	α (deg)	C_L	C_D	$C_{M\,7/4}$
1·00	60	60	0	0·3	0·009	0·0349	0
				4·55	0·287	0·0417	−0·0394
				8·8	0·574	0·0645	0·0849
				10·95	0·723	0·0958	0·1176
				13·1	0·865	0·147	0·1421
				15·2	0·970	0·219	0·1290
				17·25	1·033	0·278	0·1141
				19·25	1·045	0·338	0·1011
			−10	0·2	0·131	0·0445	0·0934
				4·4	0·138	0·0427	0·0670
				8·7	0·421	0·0541	0·0159
				10·8	0·573	0·0723	−0·0212
				13·0	0·748	0·117	−0·0694
				15·1	0·881	0·189	−0·0806
				17·2	0·964	0·245	0·0705
				19·2	0·979	0·304	−0·0640
				21·2	0·986	0·371	−0·0897
				23·2	0·982	0·425	0·1186
			20	8·55	0·287	0·0538	0·1091
				10·7	0·442	0·0643	0·0738
				12·85	0·616	0·0984	0·0918
				15·0	0·775	0·160	0·0144
				17·1	0·866	0·215	0·0136
				19·1	0·885	0·271	0·0081
				21·1	0·890	0·332	0·0350
	60	0	10	8·6	0·328	0·0384	0·0948
				10·7	0·462	0·0506	0·0665
				12·85	0·627	0·0903	0·0229
				15·0	0·745	0·152	0·0172
				17·05	0·818	0·211	0·0276
				19·05	0·831	0·265	0·0325
				21·05	0·826	0·318	0·0104
	0	60	10	0·3	−0·020	0·0198	0·0114
				4·5	0·243	0·0250	0·0098
				8·75	0·520	0·0448	0·0542
				10·9	0·665	0·0723	0·0789
				13·0	0·794	0·116	0·0978
				15·1	0·890	0·185	0·0827
				17·2	0·959	0·244	0·0689
				19·2	0·969	0·305	0·0601
				21·2	0·971	0·368	0·0857
				23·2	0·971		
0·61	60	60	−20	8·55	0·289	0·0439	0·1081
				10·7	0·440	0·0560	0·0752
				12·85	0·606	0·0914	0·0312
				14·95	0·737	0·151	0·0082
				17·05	0·824	0·209	0·0092
				19·1	0·851	0·264	0·0125
				21·05	0·847	0·323	0·0137

TABLE 9A

Lift, Drag and Pitching-Moment Coefficients with Original Letter-box Slots (slot gap = 1 per cent chord)

Complete model. Entries open. Trimming flaps 0 deg.

Slot span from tip / Semi-span	η_w = 0 deg				η_w = −10 deg			
	α (deg)	C_L	C_D	$C_{M\bar{c}/4}$	α (deg)	C_L	C_D	$C_{M\bar{c}/4}$
Flaps 0 deg V = 180 ft/sec								
0·18	6·75	0·396	0·0275	−0·0309				
	11·0	0·631	0·0653	−0·0461				
	13·1	0·750	0·107	−0·0554				
	15·15	0·833	0·158	−0·0419				
	17·2	0·885	0·226	−0·0223				
	19·2	0·893	0·278	−0·0185				
	21·2	0·890	0·336	−0·0343				
Flaps 0 deg V = 120 ft/sec								
0·18	−1·8	−0·122	0·0145	0·0084				
	2·4	0·129	0·0138	−0·0084				
	6·65	0·385	0·0268	−0·0305				
	10·9	0·629	0·0717	−0·0488				
	12·95	0·730	0·114	−0·0464				
	15·05	0·810	0·167	−0·0284				
	17·1	0·882	0·223	−0·0158				
	19·15	0·905	0·277	−0·0044				
	21·1	0·903	0·343	−0·0304				
	23·1	0·898	0·394	−0·0621				
	25·1	0·890	0·434	−0·0856				
0·29	−1·8	−0·124	0·0149	0·0076	−1·9	−0·228	0·0222	0·0792
	2·4	0·127	0·0140	−0·0069	2·3	0·021	0·0163	0·0676
	6·65	0·386	0·0268	−0·0289	6·55	0·282	0·0237	0·0443
	10·85	0·623	0·0692	−0·0459	10·8	0·529	0·0575	0·0196
	12·95	0·731	0·111	−0·0503	12·9	0·647	0·0980	0·0100
	15·05	0·832	0·169	−0·0516	15·0	0·753	0·153	0·0027
	17·1	0·897	0·223	−0·0296	17·05	0·824	0·206	0·0148
	19·15	0·910	0·277	−0·0113	19·05	0·833	0·260	0·0266
	21·15	0·907	0·341	−0·0377	21·05	0·831	0·313	0·0066
	23·15	0·904	0·390	−0·0645	23·05	0·811	0·362	−0·0171

TABLE 9A—*continued*

Slot span from tip / Semi-span	η_w = 0 deg				η_w = −10 deg			
	α (deg)	C_L	C_D	$C_{M\,\bar{c}/4}$	α (deg)	C_L	C_D	$C_{M\,\bar{c}/4}$
0·48	−1·8	−0·118	0·0156	0·0067				
	2·4	0·122	0·0144	−0·0051				
	6·65	0·376	0·0262	−0·0281				
	10·85	0·623	0·0668	−0·0455				
	12·95	0·729	0·106	−0·0525				
	15·05	0·819	0·160	−0·0389				
	17·1	0·876	0·215	−0·0080				
	19·1	0·895	0·269	0·0011				
	21·1	0·893	0·333	−0·0265				
0·73	6·65	0·374	0·0267	−0·0319	2·3	0·006	0·0180	0·0661
	10·85	0·622	0·0658	−0·0523	6·55	0·260	0·0235	0·0470
	12·95	0·730	0·104	−0·0624	10·75	0·518	0·0537	0·0175
	15·05	0·824	0·151	−0·0574	12·9	0·632	0·0872	0·0042
	17·1	0·886	0·207	−0·0210	14·95	0·738	0·133	−0·0030
	19·15	0·914	0·258	0·0021	17·05	0·810	0·190	0·0273
	21·15	0·913	0·305	0·0066	19·05	0·845	0·239	0·0462
	23·15	0·905	0·358	−0·0219	21·05	0·845	0·285	0·0472
					23·05	0·827	0·334	0·0249
Flaps 60 deg (small-chord flaps hinged in rear position). V = 120 ft/sec								
0·73					0·4	0·109	0·0505	0·0264
					4·65	0·360	0·0578	0·0040
					8·85	0·613	0·0847	−0·0207
					10·95	0·737	0·118	−0·0359
					13·05	0·845	0·162	−0·0417
					15·15	0·909	0·209	−0·0239
					17·15	0·932	0·259	−0·0004
					19·15	0·937	0·306	0·0187
					21·15	0·904	0·346	0·0273
					23·1	0·872	0·400	0·0123

TABLE 9B

Lift, Drag and Pitching-Moment Coefficients with Modified Letter-box Slots (slot gap = 2 per cent chord)

Complete model. Entries open. Trimming flaps 0 deg. $V = 120$ ft/sec.

Slot span from tip / Semi-span	η_w (deg)	α (deg)	C_L	C_D	$C_{M\,\bar{c}/4}$
Flaps 0 deg					
0·48	0	4·5	0·215	0·0185	−0·0142
		8·75	0·492	0·0386	−0·0403
		10·85	0·597	0·0569	−0·0418
		12·95	0·692	0·0870	−0·0396
		15·0	0·793	0·136	−0·0385
		17·1	0·870	0·193	−0·0206
		21·15	0·928	0·331	−0·0354
Flaps 60 deg (half-chord flaps hinged in rear position)					
0·48	0	4·7	0·456	0·0557	−0·0668
		8·95	0·703	0·0861	−0·0869
		13·15	0·906	0·155	−0·0822
		15·2	0·974	0·211	−0·0626
		17·2	1·011	0·265	−0·0380
		19·2	1·009	0·334	−0·0302
	−10	4·6	0·343	0·0578	0·0130
		8·85	0·599	0·0810	−0·0130
		10·95	0·720	0·106	−0·0230
		13·05	0·836	0·146	−0·0303
		15·15	0·915	0·202	−0·0168
		17·15	0·949	0·254	0·0050

TABLE 10

Lateral and Directional Coefficients and Derivatives

Entries open. $V = 120$ ft/sec.

Condition of model	α (deg)	C_L	β (deg)	$10^3 C_n$	$10^3 C_l$	$10^3 C_y$	n_v	l_v	y_v
No slats									
Fin off Flaps 0 deg	1·35	0·05	10	2·50	−2·43	−17·3			
			5	−1·29	−1·15	−7·8	−0·013	−0·012	0·040
			2·5	−0·57	−0·48	−3·5			
	5·6	0·31	10	−1·39	−10·43	−19·2			
			5	−0·66	−5·24	−8·9	−0·006	−0·061	0·048
			2·5	−0·26	−2·63	−4·2			
	8·45	0·49	10	−1·32	−13·89	−17·7			
			5	−0·13	−8·07	−8·8	0·001	−0·093	0·049
			2·5	0·05	−4·08	−4·3			
	13·6	0·76	10	−2·44	−19·26	−3·3			
			5	−3·21	−14·68	9·1			
			2·5	−3·57	−12·22	16·3			
			0	−3·24	−5·90	19·2			
			−2·5	−0·63	−1·74	15·6			
			−5	1·19	3·26	15·6			
			−10	2·52	11·00	21·8			
Fin on Flaps 0 deg	1·35	0·05	10	4·70	−3·42	−53·2			
			5	2·03	1·74	−24·9	0·026	−0·014	−0·147
			2·5	1·15	−0·60	−12·8			
	5·6	0·31	10	5·73	−10·28	−54·1			
			5	2·84	−5·06	−26·6	0·035	−0·057	0·154
			2·5	1·54	−2·48	−13·4			
	8·45	0·49	10	5·62	−13·84	−52·3			
			5	3·26	−7·48	−26·5	0·040	−0·091	0·151
			2·5	1·75	−3·97	−13·2			
	9·85	0·58	10	3·15	−18·27	−22·3			
			5	0·50	−10·38	−12·9			
			2·5	−0·11	−7·07	−0·8			
			0	−0·83	−3·81	10·2			
			−2·5	−2·16	0·23	23·0			
			−5	−3·59	4·88	35·5			
			−10	−4·83	11·17	59·4			
	11·35	0·66	10	1·20	−18·57	−32·9			
			5	−1·39	−11·15	−7·3			
			2·5	−2·92	−7·17	4·9			
			0	−4·08	−3·21	17·5			
			−2·5	−5·51	0·89	29·8			
			−5	−5·87	3·81	29·5			
			7·5	−2·71	3·45	—			
			−10	−1·14	10·77	53·7			
			−15	−5·58	—	—			

TABLE 10—*continued*

Condition of model	α (deg)	C_L	β (deg)	$10^3 C_n$	$10^3 C_l$	$10^3 C_y$	n_v	l_v	y_v
No slats—*cont.*									
Fin on	13·6	0·76	10	4·84	−18·73	−36·6			
Flaps 0 deg			5	0·12	−13·20	−6·3			
			2·5	−2·13	−11·18	9·4			
			0	−3·83	−5·89	21·2			
			−2·5	−2·86	−0·46	28·3			
			−5	−2·86	4·43	37·3			
			−10	−4·90	10·52	61·1			
			−15	−9·12	14·15	93·8			
			−20	−14·05	18·59	130·3			
Fin on	1·6	0·29	10	4·76	−9·05	−49·9			
Flaps 60 deg			5	2·41	−5·01	−24·3	0·030	−0·064	−0·141
(small-chord			2·5	1·32	−2·79	−12·3			
flaps hinged in									
rear position)	8·55	0·72	10	3·97	−18·52	−45·9			
			5	2·11	−10·17	−22·3	0·024	−0·110	−0·125
			2·5	1·04	−4·80	−11·0			
With 74 per cent span slats									
Fin off	18·85	1·045	10	−3·14	−38·83	11·2			
Flaps 0 deg			5	−4·19	−25·48	17·2			
			2·5	−3·82	−18·20	18·7			
			0	−3·44	−7·41	15·4			
			−2·5	−0·80	4·60	9·1			
			−5	0·22	14·39	7·9			
			−10	0·24	30·11	13·9			
Fin on	13·6	0·78	10	9·57	−19·91	−57·1			
Flaps 0 deg			5	5·10	−10·41	−29·2	0·061	−0·118	−0·162
			2·5	2·65	−5·14	−14·1			
	18·85	1·05	10	1·61	37·14	−16·3			
			5	−2·10	−26·27	4·2			
			2·5	−3·38	−18·37	13·1			
			0	−4·38	−8·34	19·0			
			−2·5	−2·53	3·62	20·9			
			−5	−2·87	13·73	24·6			
			−10	−5·65	26·48	43·8			
			−15	−11·82	40·65	71·2			
			−20	16·32					
Fin on	13·85	1·02	10	10·43	−27·01	−52·5			
Flaps 60 deg			5	5·78	14·88	−26·5	0·065	−0·178	−0·149
(small-chord			2·5	2·84	−7·76	−13·0			
flaps hinged in									
rear position)	13·7	0·86	10	10·95	−14·40	60·3			
$\eta_w =$ 0 deg			5	5·91	−7·26	−30·8	0·071	−0·087	−0·180
$\eta_w =$ −15 deg			2·5	3·12	−3·81	15·7			
With 37 per cent span slats									
Fin on	11·65	0·64	10	8·22		52·4			
Flaps 0 deg			5	4·25		25·8	0·050		−0·142
$\eta_w =$ 0 deg			2·5	2·16		12·4			

TABLE 10—*continued*

Condition of model	α (deg)	C_L	β (deg)	$10^3\,C_n$	$10^3\,C_l$	$10^3\,C_y$	n_v	l_v	y_v
With 37 per cent span slats—*cont.* Fin on Flaps 0 deg $\eta_w = 0$ deg	13·8	0·76	10 5 2·5	6·94 4·07 2·07		−46·2 −24·0 −12·1	0·047		−0·139
	15·05	0·82	10 5 2·5	7·32 3·71 1·90	−23·03 −12·08 5·98	−46·4 −22·0 −11·2	0·044	−0·137	0·128
	16·6	0·89	10 5 2·5 0 −2·5 −5 −7·5 −10 −15	6·76 2·57 0·54 1·47 −3·45 5·20 6·30 7·41 −11·95		−41·5 −14·2 1·8 10·5 21·8 34·0 45·5 58·4 88·3			
	18·15	0·94	10 5 2·5 0 2·5 −5 7·5 10 15	5·51 1·57 −0·46 1·93 3·09 −3·62 4·09 −6·23 −9·74		−40·6 −14·0 1·1 14·2 25·2 35·8 45·6 59·3 85·2			
Fin on Flaps 60 deg (small-chord flaps hinged in rear position) $\eta_w = 0$ deg	11·05	0·84	10 5 2·5	8·60 4·53 2·26	25·09 −13·70 7·62	−50·7 −25·6 −12·3	0·052	0·175	0·141
	15·25	1·04	10 5 2·5	7·91 4·55 2·34	26·34 12·32 −6·19	−49·6 25·5 −13·7	0·054	0·142	0·157
	16·8	1·06	10 5 2·5 0 2·5 5 10	4·47 1·67 0·53 2·75 4·33 4·82 8·11	−29·53 −18·39 14·75 8·83 5·04 2·00 15·74	−42·7 14·3 1·8 16·5 30·9 38·9 62·1			
	18·25	1·05	10 5 2·5 0 2·5 5 10	3·44 0·02 1·14 2·09 2·08 −1·83 −4·56	26·89 19·29 17·10 15·07 10·65 2·61 10·79	34·1 8·8 5·1 15·2 26·6 37·1 59·0			

TABLE 10—*continued*

Condition of model	α (deg)	C_L	β (deg)	$10^3\ C_n$	$10^3\ C_l$	$10^3\ C_y$	n_v	l_v	y_v
With 37 per cent span slats—*cont.*									
Fin on Flaps 60 deg $\eta_w = -15$ deg	10·9	0·68	10	8·99	−11·69	−56·5			
			5	4·53	−5·57	−28·5	0·054	−0·078	−0·156
			2·5	2·37	−3·40	−13·6			
	14·1	0·88	10	6·52	−20·72	−41·7			
			5	3·65	−12·30	−18·9			
			2·5	1·74	−7·91	−7·2			
			0	−0·68	−3·60	5·2			
			−2·5	−3·19	1·38	19·7			
			−5	−5·73	6·33	33·3			
			−10	−9·93	15·12	59·8			
	15·15	0·92	10	6·82	−20·41	−43·7			
			5	3·13	−12·06	−18·1			
			2·5	0·82	−8·15	−4·1			
			0	−1·62	−4·88	11·0			
			−2·5	−4·32	−0·61	25·2			
			−5	−6·74	3·19	38·1			
			−10	−9·73	14·35	61·7			
			−15	−14·55	22·15	94·9			
$\eta_w = -15$ deg Trimming flaps −15 deg (split flaps deflecting with trimming flaps)	10·8	0·55	10	7·99	−8·21	−56·6			
			5	4·04	−4·53	−28·4	0·049	−0·053	−0·163
			2·5	2·15	−2·33	−14·3			
	15·05	0·80	10	6·20	−19·80	−42·7			
			5	3·51	−12·26	−19·2			
			2·5	1·57	−8·41	−6·7			
			0	−0·77	−3·86	6·6			
			−2·5	−3·19	0·65	20·5			
			−5	−5·50	5·17	33·6			
			−10	−9·36	13·35	60·7			
			−15	−12·90	20·28	91·5			
Fin on Flaps 60 deg $\eta_w = -15$ deg Trimming flaps −15 deg	16·6	0·90	10	6·12	−21·44	−42·9			
			5	2·17	−13·56	−14·6			
			2·5	0·09	−10·07	−2·4			
			0	−1·82	−6·26	11·6			
			−2·5	−3·87	−1·02	23·8			
			−5	−5·79	3·37	38·0			
			−10	−8·49	13·51	62·8			
			−15	−12·83	20·36	91·6			

TABLE 11

Elevon power

Complete Model. Entries Open. Trimming Flaps 0 deg. $V = 120$ ft/sec.

Condition of model	α (deg)	η_w (deg)	Port elevon only				Port and starboard elevons
			ΔC_L	$10^3 \Delta C_n$	$10^3 \Delta C_l$	$10^3 \Delta C_Y$	$\Delta C_{M\,\bar{c}/4}$
No slats Flaps 0 deg	1·35	15	0·097	2·44	28·22	0·37	0·1242
		15	0·087	1·84	26·79	2·88	0·1220
		20	0·113	3·48	34·74	4·60	0·1588
		25	0·135	5·92	41·12	7·26	0·1850
	5·6	15	0·076	2·67	25·09	1·73	0·1020
		15	0·085	1·39	25·77	6·74	0·1226
		20	0·114	2·76	34·37	9·69	0·1600
		25	0·132	4·67	38·52	12·89	0·1742
	8·45	15	0·078	3·18	21·90	1·19	0·0952
		15	0·070	0·26	23·93	8·21	0·1084
		20	0·100	1·32	31·96	10·66	0·1448
		25	0·118	3·43	38·35	15·16	0·1706
	13·6	15	0·067	5·86	15·41	1·1	0·0716
		15	0·066	2·23	19·41	3·1	0·0834
		20	0·086	2·35	25·18	5·2	0·1116
		25	0·103	2·13	30·24	7·5	0·1328
With 74 per cent span slats Flaps 0 deg	13·6	15	0·065	3·97	20·87	3·56	0·0912
		15	0·082	0·86	25·60	10·04	0·1084
		20	0·111	0·33	33·74	14·24	0·1430
		25	0·133	0·72	40·33	18·84	0·1718
Flaps 60 deg (small-chord flaps hinged in rear position)	13·85	15		4·19	15·25	1·0	
		15		1·05	24·35	9·1	

TABLE 12

Rudder Power

Complete model. Entries open. Plain wing. Split flaps 0 deg.
Trimming flaps 0 deg. $V = 120$ ft/sec.

α (deg)	C_L	ζ (deg)	$10^3 \Delta C_n$	$10^3 \Delta C_Y$
1·35	0·05	20	7·61	32·8
		15	5·68	23·9
		10	3·57	15·3

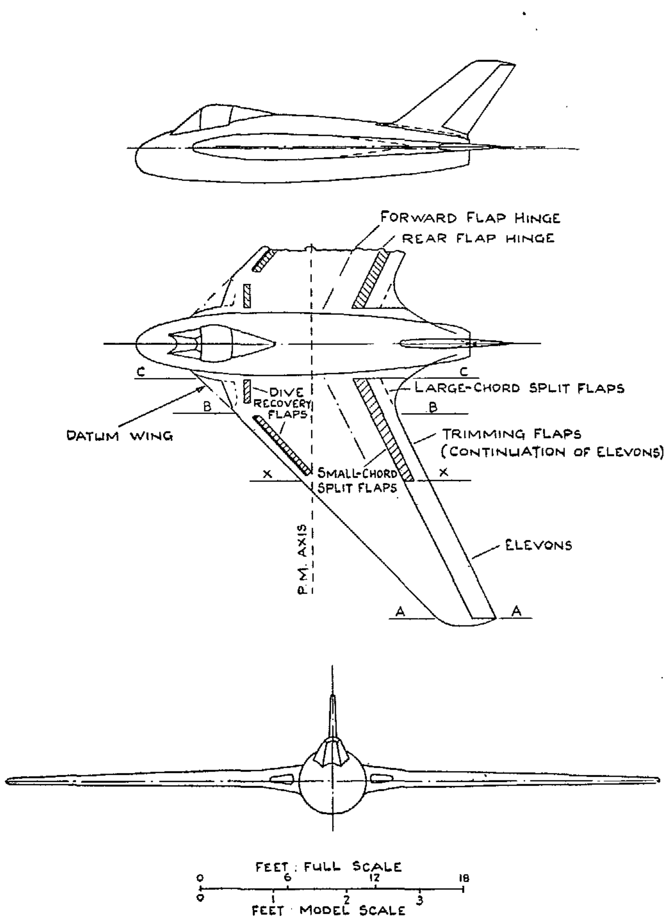

FIG. 1. Wind-tunnel model.

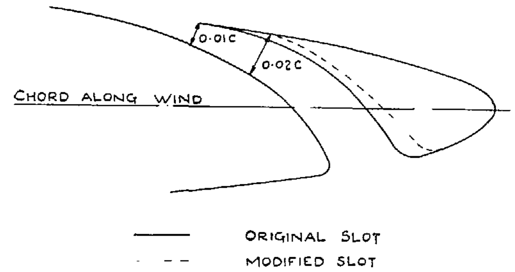

FIG. 2a. Details of letter-box slots.

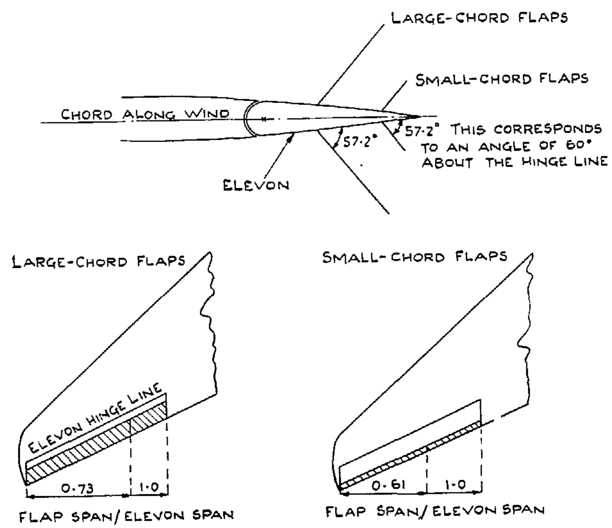

FIG. 2b. Details of double split flaps.

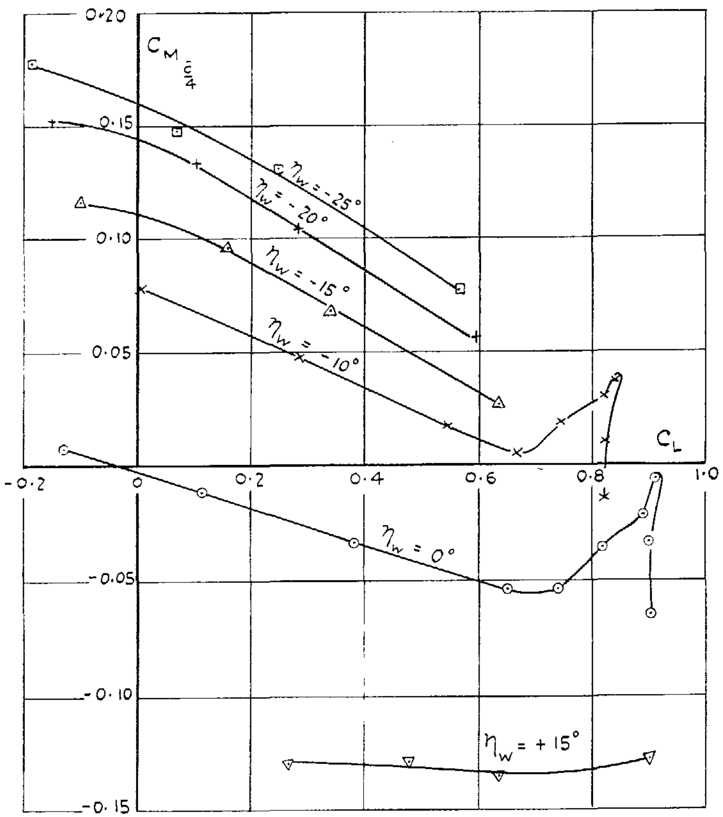

FIG. 3. Pitching-moment coefficients. Flaps 0 deg. η_w = +15 deg, −15 deg, −20 deg, −25 deg (η_w = elevon angle measured along wind).

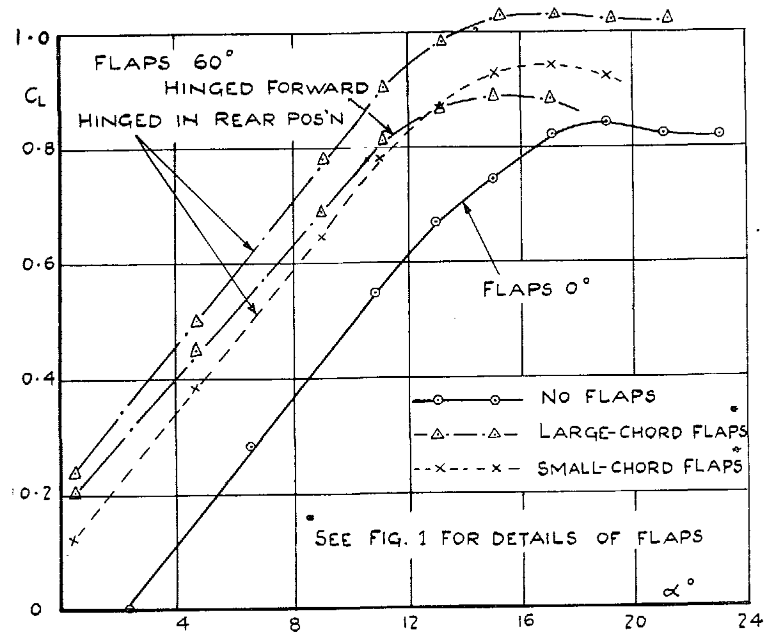

FIG.4 LIFT COEFFICIENTS η_w = -10°

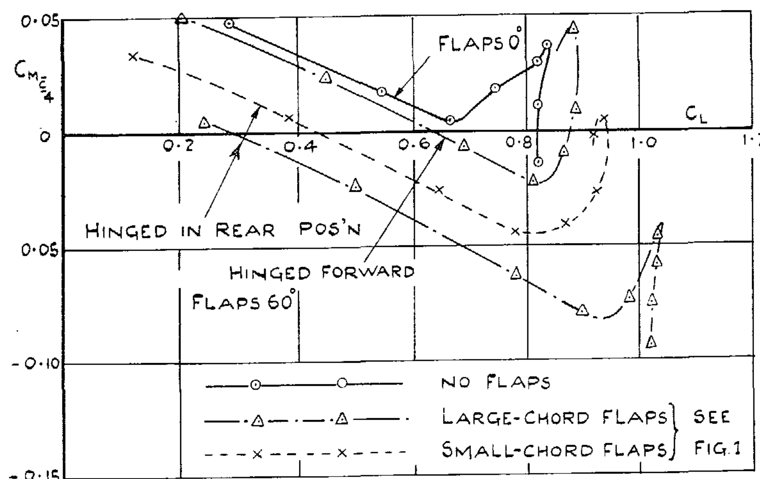

FIG 5. PITCHING-MOMENT COEFFICIENTS η_w = -10°

FIGS. 4 and 5. Effect of split flaps.

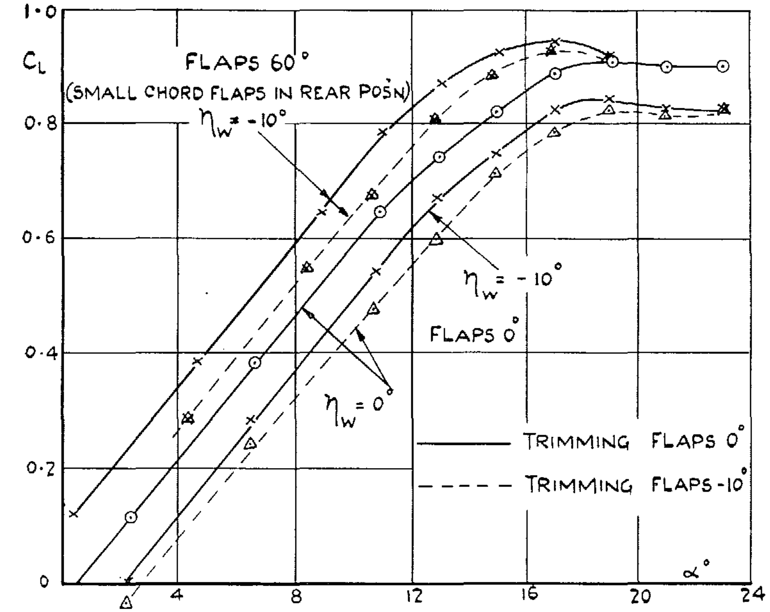

FIG. 6 LIFT COEFFICIENTS.

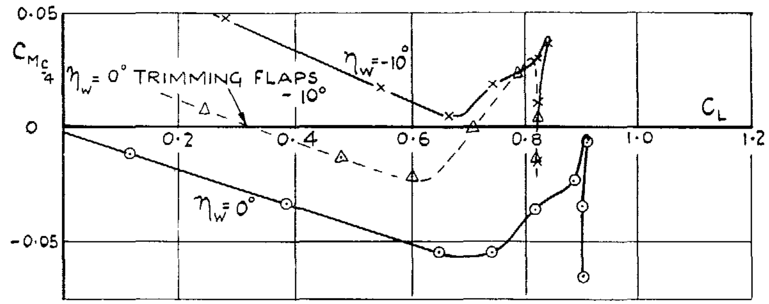

FIG. 7. PITCHING MOMENTS. FLAPS 0°

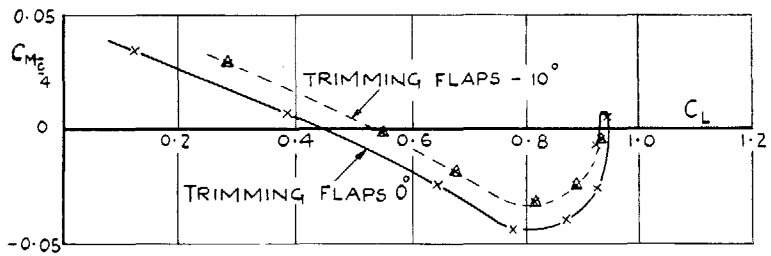

FIG. 8. PITCHING MOMENTS. SMALL-CHORD FLAPS 60°, $\eta_w = -10°$

FIGS. 6, 7 and 8. Effect of trimming flaps.

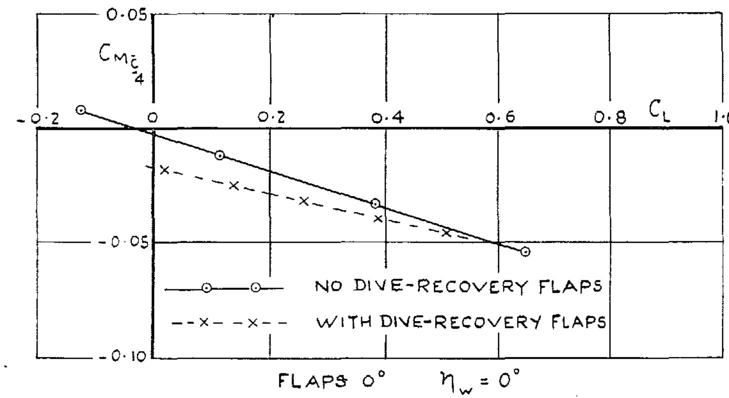

FIG. 9. Effect of dive-recovery flaps.

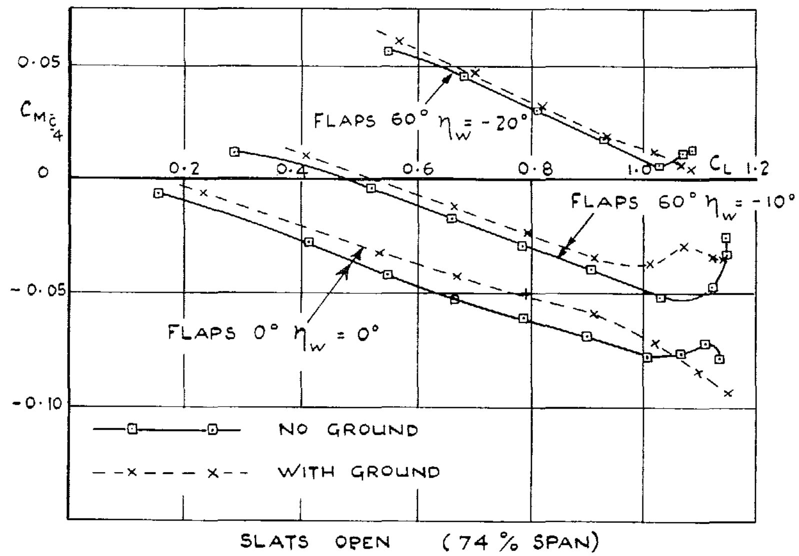

FIG. 10. Effect of ground.

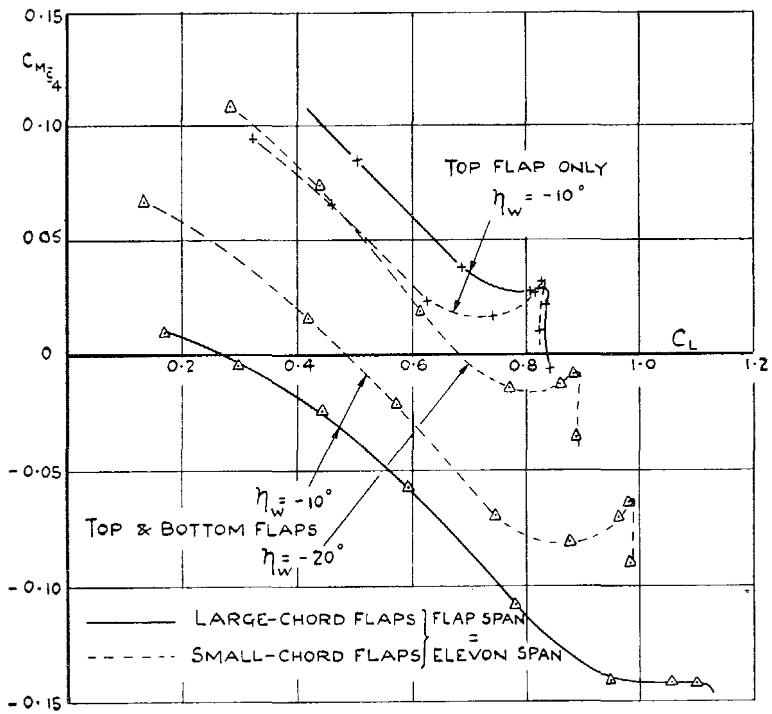

FIG. 11. Pitching moments with double split flaps.

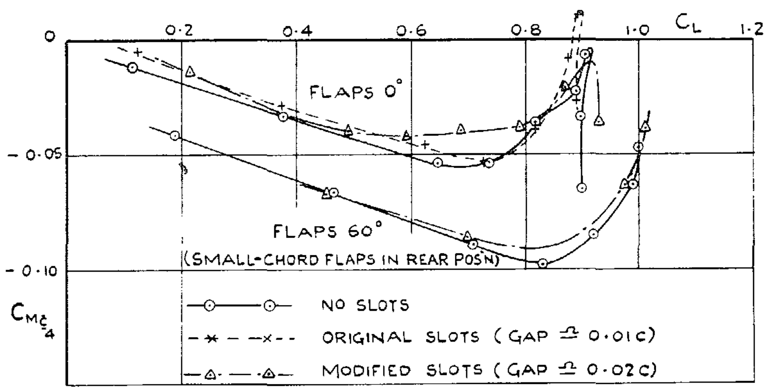

FIG. 12. Pitching moments with letter-box slots. $\eta_w = 0$ deg.

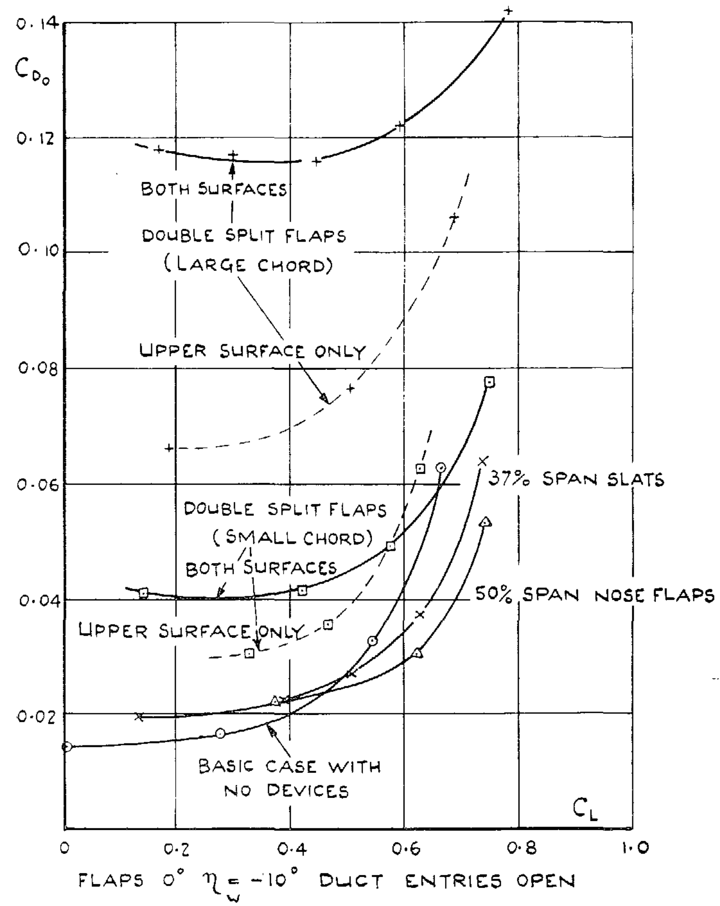

FIG. 13. Profile-drag coefficients with and without anti-tip-stalling devices.

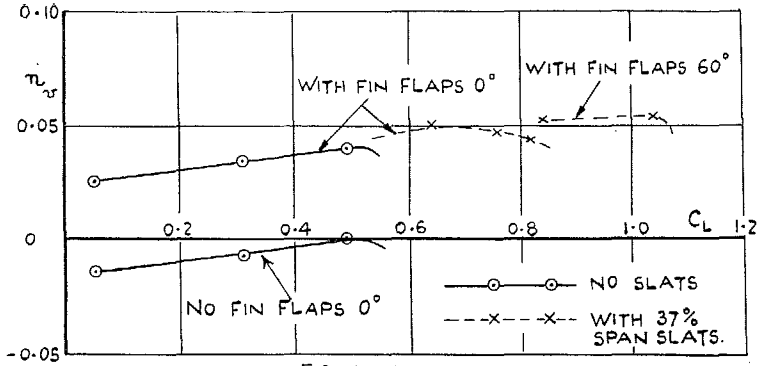

FIG. 14. n_v vs. C_L

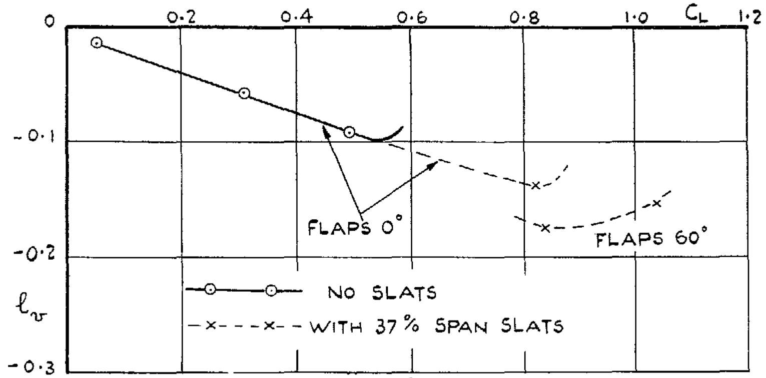

FIG. 15. l_v vs. C_L

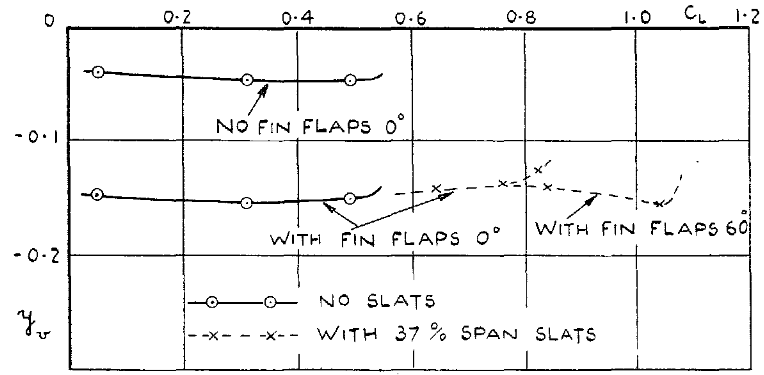

FIG. 16. y_v vs. C_L

FIGS. 14, 15 and 16. Lateral derivatives.

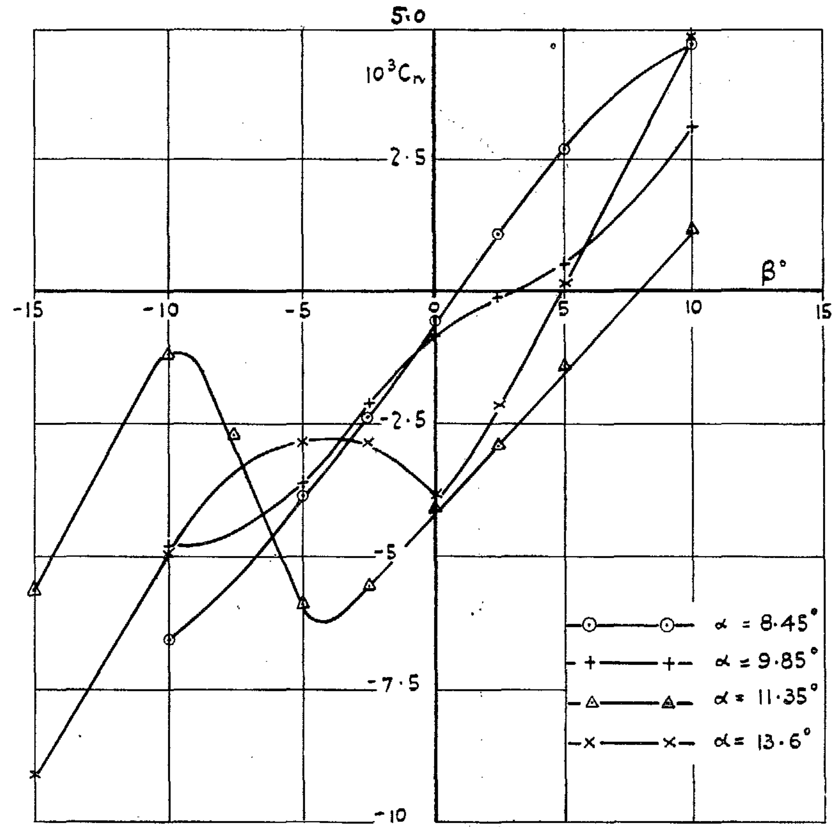

FIG. 17. Yawing-moment curves. No slats.

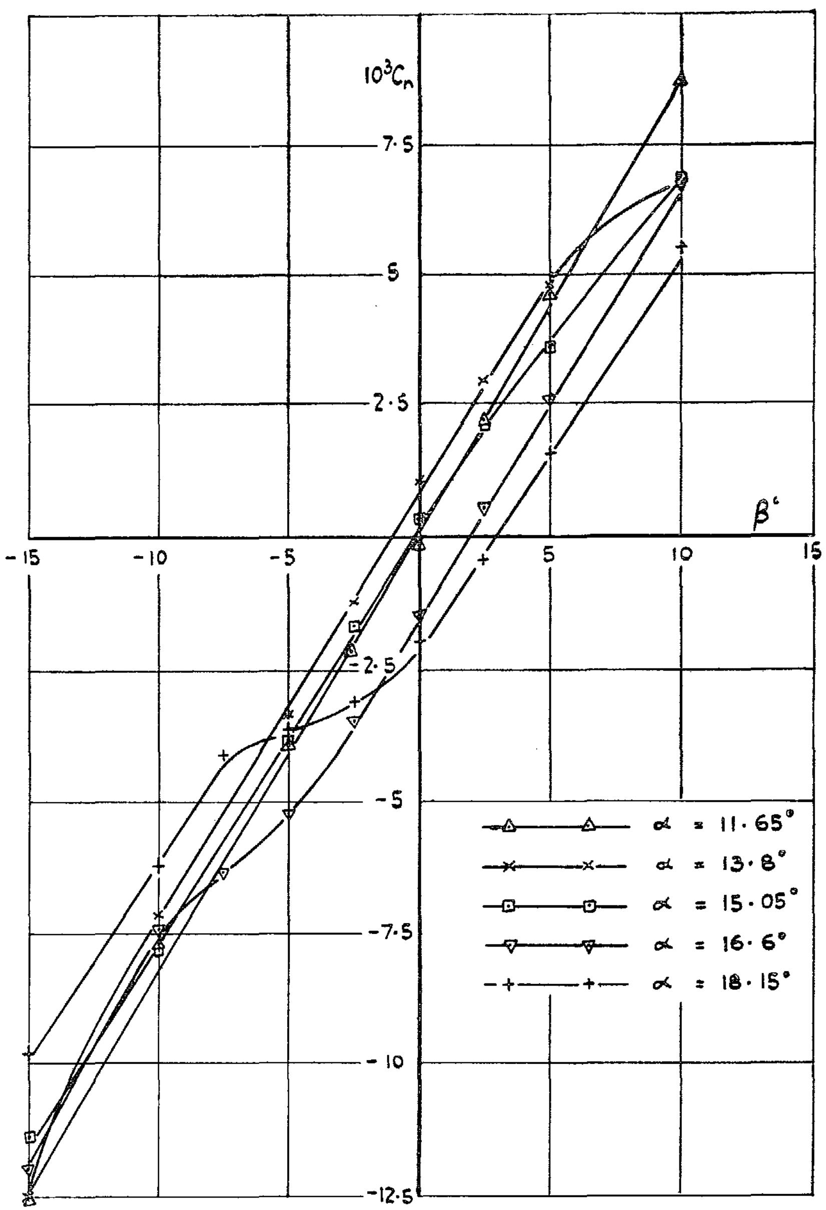

FIG. 18. Yawing-moment curves with 37 per cent span slats.

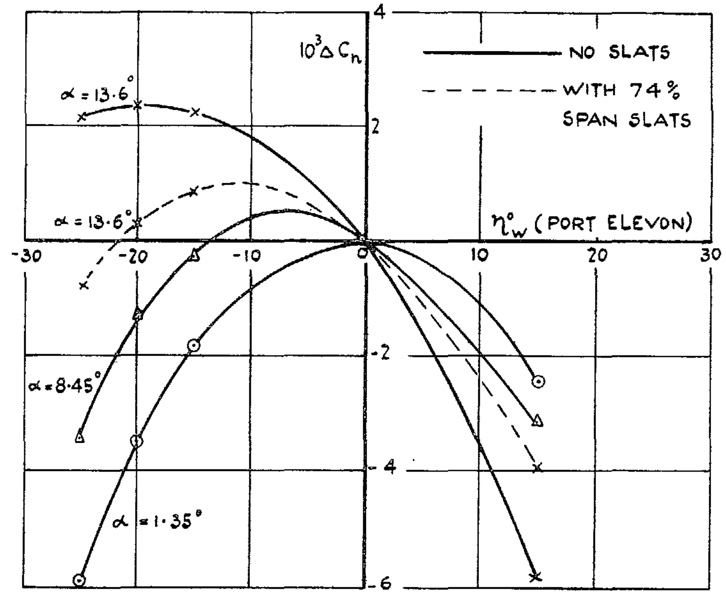

FIG. 19. YAWING MOMENTS FLAPS 0°

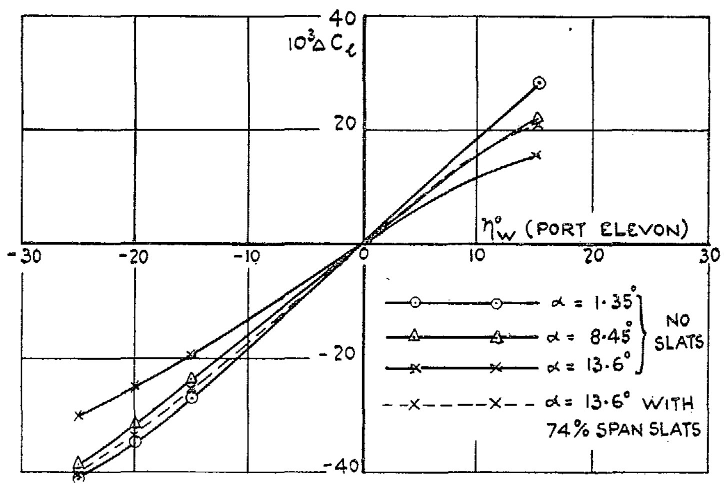

FIG. 20. ROLLING MOMENTS. FLAPS 0°

FIGS. 19 and 20. Elevon power (η_w = elevon angle measured along wind).

(6135) Wt. 17/680 K.7 3/56 H.P.Co. 34-261

PRINTED IN GREAT BRITAIN

Publications of the Aeronautical Research Council

ANNUAL TECHNICAL REPORTS OF THE AERONAUTICAL RESEARCH COUNCIL (BOUND VOLUMES)—

1938 Vol. I. Aerodynamics General, Performance, Airscrews. 50*s*. (51*s*. 8*d*.)
Vol. II. Stability and Control, Flutter, Structures, Seaplanes, Wind Tunnels, Materials. 30*s*. (31*s*. 8*d*.)

1939 Vol. I. Aerodynamics General, Performance, Airscrews, Engines. 50*s*. (51*s*. 8*d*.)
Vol. II. Stability and Control, Flutter and Vibration, Instruments, Structures, Seaplanes, etc. 63*s*. (64*s*. 8*d*.)

1940 Aero and Hydrodynamics, Aerofoils, Airscrews, Engines, Flutter, Icing, Stability and Control, Structures, and a miscellaneous section. 50*s*. (51*s*. 8*d*.)

1941 Aero and Hydrodynamics, Aerofoils, Airscrews, Engines, Flutter, Stability and Control, Structures. 63*s*. (64*s*. 8*d*.)

1942 Vol. I. Aero and Hydrodynamics, Aerofoils, Airscrews, Engines. 75*s*. (76*s*. 8*d*.)
Vol. II. Noise, Parachutes, Stability and Control, Structures, Vibration, Wind Tunnels. 47*s*. 6*d*. (49*s*. 2*d*.)

1943 Vol. I. Aerodynamics, Aerofoils, Airscrews. 80*s*. (81*s*. 8*d*.)
Vol. II. Engines, Flutter, Materials, Parachutes, Performance, Stability and Control, Structures. 90*s*. (91*s*. 11*d*.)

1944 Vol. I. Aero and Hydrodynamics, Aerofoils, Aircraft, Airscrews, Controls. 84*s*. (86*s*. 9*d*.)
Vol. II. Flutter and Vibration, Materials, Miscellaneous, Navigation, Parachutes, Performance, Plates and Panels, Stability, Structures, Test Equipment, Wind Tunnels. 84*s*. (86*s*. 9*d*.)

ANNUAL REPORTS OF THE AERONAUTICAL RESEARCH COUNCIL—

1933–34	1*s*. 6*d*. (1*s*. 8½*d*.)	1937	2*s*. (2*s*. 2½*d*.)
1934–35	1*s*. 6*d*. (1*s*. 8½*d*.)	1938	1*s*. 6*d*. (1*s*. 8½*d*.)
April 1, 1935 to Dec. 31, 1936	4*s*. (4*s*. 5½*d*.)	1939–48	3*s*. (3*s*. 3½*d*.)

INDEX TO ALL REPORTS AND MEMORANDA PUBLISHED IN THE ANNUAL TECHNICAL REPORTS, AND SEPARATELY—

April, 1950 . . . . . . R. & M. No. 2600 2*s*. 6*d*. (2*s*. 7½*d*.)

AUTHOR INDEX TO ALL REPORTS AND MEMORANDA OF THE AERONAUTICAL RESEARCH COUNCIL—

1909–January, 1954 . . . R. & M. No. 2570 15*s*. (15*s*. 5½*d*.)

INDEXES TO THE TECHNICAL REPORTS OF THE AERONAUTICAL RESEARCH COUNCIL—

December 1, 1936 — June 30, 1939	R. & M. No. 1850	1*s*. 3*d*. (1*s*. 4½*d*.)
July 1, 1939 — June 30, 1945	R. & M. No. 1950	1*s*. (1*s*. 1½*d*.)
July 1, 1945 — June 30, 1946	R. & M. No. 2050	1*s*. (1*s*. 1½*d*.)
July 1, 1946 — December 31, 1946	R. & M. No. 2150	1*s*. 3*d*. (1*s*. 4½*d*.)
January 1, 1947 — June 30, 1947	R. & M. No. 2250	1*s*. 3*d*. (1*s*. 4½*d*.)

PUBLISHED REPORTS AND MEMORANDA OF THE AERONAUTICAL RESEARCH COUNCIL—

Between Nos. 2251–2349	R. & M. No. 2350	1*s*. 9*d*. (1*s*. 10½*d*.)
Between Nos. 2351–2449	R. & M. No. 2450	2*s*. (2*s*. 1½*d*.)
Between Nos. 2451–2549	R. & M. No. 2550	2*s*. 6*d*. (2*s*. 7½*d*.)
Between Nos. 2551–2649	R. & M. No. 2650	2*s*. 6*d*. (2*s*. 7½*d*.)

Prices in brackets include postage

HER MAJESTY'S STATIONERY OFFICE

York House, Kingsway, London, W.C.2; 423 Oxford Street, London, W.1 (Post Orders: P.O. Box 569, London, S.E.1); 13a Castle Street, Edinburgh 2; 39 King Street, Manchester 2; 2 Edmund Street, Birmingham 3; 109 St. Mary Street, Cardiff; Tower Lane, Bristol 1; 80 Chichester Street, Belfast *or through any bookseller*

S.O. Code No. 23-2843

R. & M. No. 2843